Mapping of Disulfide Bridges in Antifreeze Proteins from Overwintering Larvae of the Beetle *Dendroides canadensis*†

Ning Li,‡ Bakshy A. K. Chibber,§ Francis J. Castellino,§ and John G. Duman*,‡

Department of Biological Sciences and Department of Chemistry and Biochemistry, University of Notre Dame, Notre Dame, Indiana 46556

Received November 20, 1997; Revised Manuscript Received March 3, 1998

ABSTRACT: Antifreeze proteins (AFPs) have been identified in certain high-latitude marine fish, insects and other terrestrial arthropods, and plants. Despite considerable structural variation, the mechanisms of their noncolligative antifreeze activity are probably quite similar. AFPs hydrogen bond onto the surface of potential seed ice crystals at preferred growth sites, thereby preventing growth of the crystals. AFPs from overwintering larvae of the beetle *Dendroides canadensis* are among the most active AFPs. These 8.7-kDa proteins consist of seven 12- or 13-mer repeating units. Their most striking feature is the location of cysteines every six residues throughout their length. Consequently, identification of the disulfide linkages of these cysteines is essential to understanding the structure of these AFPs. This study demonstrated that all of the 16 Cys residues in the *Dendroides* AFPs are disulfide bridged. All of the seven 12- or 13-mer repeats have internal disulfide bridges, and in all but the first repeat the Cys residues at positions 1 and 7 of the repeats are linked. In repeat 1 the Cys at position 1 is linked to the Cys at position 10, rather than the Cys at position 7 as in the other repeats, and the Cys at position 7 of the first repeat is linked to a Cys at position 4 of the second repeat. The disulfide bridges probably function to position the hydrophilic side chains of serine and threonine residues so that they hydrogen bond with ice.

Antifreeze proteins (AFPs),[1] also known as thermal hysteresis proteins (THPs), were first identified in polar marine fishes where they function to depress the freezing point of the body fluids of the hypo-osmoregulating fish below that of seawater (*1*−*3*). AFPs are also present in many terrestrial arthropods including insects (*4*, *5*), spiders (*6*, *7*), mites (*8*) and centipedes (*9*, *10*). More recently, thermal hysteresis proteins have been identified in many plants (*11*−*15*), fungi, and bacteria (*14*). In overwintering larvae of the beetle *Dendroides canadensis* the AFPs function to inhibit inoculative freezing across the cuticle by external ice and to inhibit ice nucleators both in the gut and in hemolymph of this freeze-avoiding insect (*16*, *17*).

AFPs depress the nonequilibrium freezing point of water by a noncolligative mechanism while not lowering the melting point, thereby producing a difference between the freezing and melting points which has been termed thermal hysteresis (*1*, *18*). In general, the magnitude of the thermal hysteresis activity depends on the specific activity and concentration of the particular AFP (*5*). While the structures of the various AFPs differ considerably, their mechanism of freezing point depression depends on their ability to adsorb onto the surface of potential seed ice crystals, probably via hydrogen bonding. This forces crystal growth into highly curved (high free energy) fronts, rather than the preferred low-curvature (low free energy) fronts. Therefore, growth is halted by the Kelvin effect until the temperature is lowered sufficiently (*19*−*21*). While details of the adsorption mechanism are somewhat uncertain, considerable data are now available on the fish AFPs (*22*), and a lattice match between polar side groups of the AFP and water molecules in the ice crystal appears likely.

Four basic categories of fish AFPs have been identified, one glycoprotein type with considerable repeat structure and three protein types with varying levels of repeating structure, presumably to allow efficient hydrogen bonding to the crystal lattice of ice. (For reviews, see refs *2* and *3*). AFPs 1 and 2 of the larvae of the beetle *Dendroides canadensis* are ∼8.7 kDa in molecular mass and have 83 and 84 amino acid residues, respectively, arranged in seven 12- or 13-mer repeat units with the consensus sequence

$$\text{-C-T-}X_3\text{-S-}X_5\text{-}X_6\text{-C-}X_8\text{-}X_9\text{-A-}X_{11}\text{-T-}X_{13}\text{-}$$

where X_3 and X_{11} tend toward charged residues, X_5 tends toward threonine or serine, X_6 tends toward asparagine or aspartate, X_9 tends toward asparagine or lysine, and X_{13} tends toward alanine (*23*). The complete sequences of *Dendroides canadensis* AFP-1 and AFP-2 arranged in the seven repeat units (A−G) are shown in Figure 1. Throughout most of the sequence of the proteins, every sixth residue is a cysteine

† Supported by Air Force Office of Scientific Research Grant F49620-95-1-0188 (J.G.D.).

‡ Department of Biological Sciences.

§ Department of Chemistry and Biochemistry.

[1] Abbreviations: A, alanine; AFP, antifreeze protein; C, cysteine; CDAP, 1-cyano-4-(dimethylamino)pyridinium tetrafluoroborate; D, aspartate; E, glutamate; F, phenylalanine; G, glycine; H, histidine; HPLC, high-pressure liquid chromatography; I, isoleucine; K, lysine; L, leucine; MALDI-TOF, matrix-assisted laser desorption ionization time-of-flight; N, asparagine; P, proline; Q, glutamine; R, arginine; S, serine; T, threonine; TCEP, Tris(2-carboxyethyl)phosphine hydrochloride; TFA, trifluoroacetic acid; THP, thermal hysteresis protein; V, valine; W, tryptophan; Y, tyrosine.

S0006-2960(97)02853-5 CCC: $15.00
Published on Web 04/16/1998

Repeat	Position 1	2	3	4	5	6	7	8	9	10	11	12	13	
A	pQ	C	T	G	G	S	D	C	R	S	C	T	V	S 14
B		C	T	D	C	Q	N	C	P	N	A	R	T	A 27
C		C	T	R	S	S	N	C	I	N	A	L	T	- 39
D		C	T	D	S	Y	D	C	H	N	A	E	T	- 51
E		C	T	R	S	T	N	C	Y	K	A	K	T	- 63
F		C	T	G	S	T	N	C	Y	E	A	-	T	A 75
G		C	T	D	S	T	G	C	P					83

FIGURE 1: Amino acid sequence of *D. canadensis* AFP-1 arranged to demonstrate the seven 12- or 13-mer repeating units (A−G) present in the protein (*23*). The two positions where AFP-2 differs from AFP-1 are identified by underlining. These are positions C8 (N for I) and F_{11} (an additional T is present in DAFP-2.). Note that the N-terminus is pyroglutamine. Numbers on the right indicate the residue number of the last position of the various repeats.

(positions 1 and 7 of the 12−13-mer repeat units). In addition, repeats A and B (amino terminus) each have one additional cysteine residue, repeat A at position 10 and repeat B at position 4. Consequently, it was critical for the eventual complete understanding of the structure of the *D. canadensis* AFP that it be determined whether these 16 cysteines are free or whether they are involved in disulfide bridges, and if the latter, to identify the linkages of the cystines. The results of these studies are reported in this paper.

EXPERIMENTAL PROCEDURES

Purification of Dendroides AFP. *Dendroides canadensis* AFP was purified as described previously (*24*) with the following modifications. Pooled hemolymph from *Dendroides* was fractionated on a polyacrylamide P-30 (medium fine) column (120 × 2 cm, 50 mM Tris-HCl and 100 mM NaCl, pH 7.0). Fractions were collected and assayed for antifreeze activity by measuring thermal hysteresis activity using the capillary freezing−melting point technique (*18*). Fractions with antifreeze activity were further separated by ion-exchange chromatography on a DEAE-Sepharose CL-6B anion-exchange column (25 × 3 cm, 25 mM Tris-HCl, pH 7.0 and 0−500 mM NaCl). Fractions with thermal hysteresis activity were identified and purified by HPLC on a Vydac Protein & Peptide C18 reverse-phase HPLC column (218TP54, 4.6 × 250 mm) using an acetonitrile gradient of 10−40% in 60 min, with a flow rate of 1 mL/min in the presence of 0.1% trifluoroacetic acid, at room temperature. The major peak, which contains AFP-1 and AFP-2 (Figure 2), was collected, dried by vacuum centrifugation, and stored at −20 °C.

General Strategy. The first question to be addressed was, how many of the 16 Cys residues are involved in disulfide bridges, and how many are free cysteines. The strategy for the determination of the disulfide bridges was to obtain as many peptide fragments as possible by treating with the nonspecific protease pepsin. An advantage of using pepsin is that its optimum pH is 2.0, which will prevent disulfide exchange during incubation. After each fragment was purified to homogeneity, they were fully reduced and separated by RP-HPLC. Identification of each peptide fragment was facilitated by obtaining the first 5−6 cycles of sequence along with the mass data and comparing them with the known amino acid sequence (Figure 1) (*23*). If only one peptide fragment is obtained after reduction and there are only two cysteines in this peptide sequence, this indicates that there is one intrachain disulfide bridge. On the other hand, if two peptide fragments are obtained after reduction and each has two cysteines in its sequence, then these two peptides may form interchain disulfide bridges, but only if these two peptides show a 1:1 molar ratio. Otherwise, these two peptides could be copurified, with each having an intrachain disulfide bridge. This could be verified by MALDI-TOF mass spectometry data of the unreduced peptide.

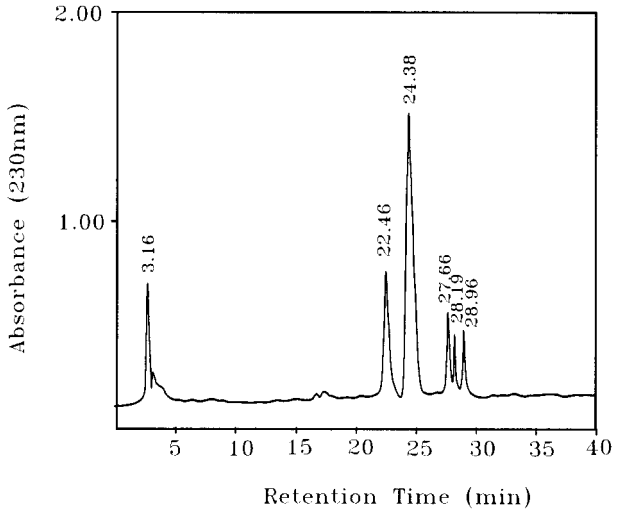

FIGURE 2: Reverse-phase HPLC of the AFP fraction from DEAE-Sepharose CL6B anion-exchange chromatography. Column: Vydac Protein & Peptide C18 (218TP54, 4.6 × 250 mm). Solvent system: solvent A, 0.1% trifluoroacetic acid in water; solvent B, 1% trifluoroacetic acid in acetonitrile. Gradient: 10−40% B in 60 min. Flow rate, 1 mL/min. Absorbance was measured at 230 nm. The major peak (24.38) is AFP-1 + AFP-2.

Assay for Free Cysteine. A mixture of native *Dendroides* AFP-1 and AFP-2 (40 μg) was denatured in 0.2 M Tris-HCl with 6 M guanidine-HCl and treated with 0.1 M iodoacetic acid at pH 8.8 to alkylate any free cysteine residues. After incubation at 37 °C for 4 h in the dark, the sample was purified by reverse-phase HPLC (C18 column) and dried. The molecular mass of the native AFP was then compared to that of the above treated AFP by MALDI-TOF mass spectrometry.

Cleavage of Native AFP and Separation of Peptides. *Dendroides* AFP-1 and AFP-2 (3 mg/mL) were digested with pepsin in H_2O−HCl (pH 2.0) with an enzyme-to-substrate ratio of 1:20 (w/w) at 37 °C for 28 h.

The above digestion mixture was separated using a Rainin reverse-phase C18 HPLC column (4.6 × 100 mm) with a 0.1% trifluoroacetic acid−acetonitrile gradient of 5−30% in 40 min. Peaks not well resolved were further purified to homogeneity using the same column and a more shallow elution gradient.

Complete Reduction of Disulfide Bridges. Each purified peptide was incubated in 0.1 M sodium citrate, pH 3.0, with 15 mM TCEP [Tris(2-carboxyethyl)phosphine hydrochloride] at 60 °C for 20 min to fully reduce any disulfides. The reduced peptides were separated by the same methods as described above for the separation for peptides.

Automated Edman Sequencing. Automated Edman sequencing was performed on a Beckman LF 3000 protein sequencer.

Mass Spectrometry Analysis. MALDI-TOF mass spectra were obtained on a PerSeptive Biosystems/Voyager-DE

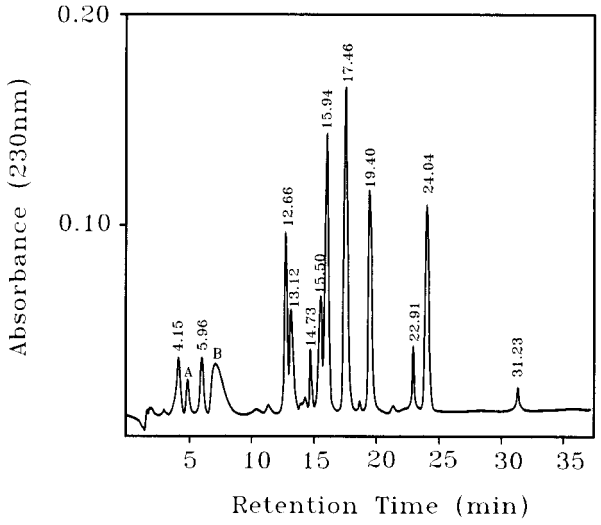

FIGURE 3: Reverse-phase HPLC of the peptide fraction from digestion of AFP by pepsin. Column: C18, 4.6 mm i.d. × 10 cm, Rainin. Solvent system: solvent A, 0.1% trifluoroacetic acid in water; solvent B, 1% trifluoroacetic acid in acetonitrile. Gradient: 5−30% B in 40 min. Flow rate, 1 mL/min. Absorbance was measured at 230 nm.

MALDI-TOF mass spectrometer. Matrix (α-cyano-4-hydroxycinnamic acid) was prepared as a saturated solution in 1:1 (v/v) water−acetonitrile with 0.1% TFA. Peptide or protein sample was dissolved in ddH_2O−TFA at pH 3.0. A 0.5-μL aliquot of sample solution was then mixed with an equal volume of the saturated matrix solution in a sample plate and allowed to air-dry before analysis. All samples were run in linear mode with a 20-kV accelerating voltage, a 18.6-kV secondary grid voltage, and a 15-V guide wire voltage.

Partial Reduction of Disulfides, Cyanylation of Free Cysteines, and Base Cleavage. The technique developed by Wu et al. (*25*) was employed to analyze disulfide linkage patterns in highly bridged small peptides with closely spaced cysteine residues, as follows. After peptides were solubilized in 10 μL of 0.1 M citrate buffer (pH 3.0), partial reduction was performed by adding 1 equivalent of TCEP for the cysteine content in the peptide, followed by incubation at room temperature for 15 min. Cyanylation of the nascent sulfhydryl groups was achieved by adding a 20-fold molar excess of 1-cyano-4-(dimethylamino)pyridinium tetrafluoroborate solution over the total cysteine content and incubating at room temperature for another 15 min. Partially reduced and cyanylated species were separated by reverse-phase HPLC as described above. Peptide isomers were collected and analyzed by MALDI-TOF. Fractions identified as having only one disulfide were reduced and dried for base cleavage. Cleavage of the peptide chain was performed by adding 100 μL of 1 M NH_4OH (pH 12.0) and incubating at room temperature for 1 h. After removal of excess ammonium hydroxide by vacuum centrifugation, the truncated peptides, still linked by residual disulfide bridges, were fully reduced by reacting with 100 μL of 0.15 mM TCEP at 37 °C for 30 min at pH 3. Samples were dried for MALDI-TOF analysis.

RESULTS

Previous determination of the sequences of *Dendroides canadensis* AFP-1 and -2 showed that there are 16 cysteine

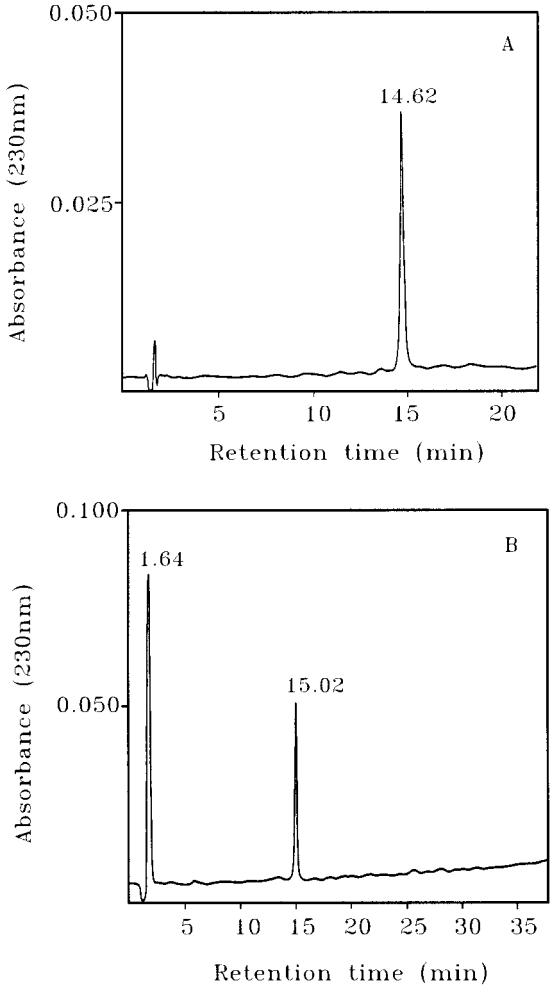

FIGURE 4: (A) Repurification of peptide 14.73. Peptide 14.73 from Figure 3 was rechromatographed by reverse-phase HPLC on a Rainin C18 column at a flow rate of 1.0 mL/min with a 5−30% linear gradient of solvent B in 40 min, where solvent A was 0.1% TFA in water and solvent B was 0.1% TFA in acetonitrile. Absorbance was measured at 230 nm. (B) Analysis of peptide 14.62 from Figure 4A by RP-HPLC after reduction. Peptide 14.62 from Figure 3 was dried and reduced in 100 μL of 0.2 M sodium citrate, pH 3.0, with 15 mM TCEP at 60 °C for 20 min, after which it was rechromatographed by reverse-phase HPLC on a Rainin C18 column at a flow rate of 1.0 mL/min with a 5−30% linear gradient of solvent B in 40 min, where solvent A was 0.1% TFA in water and solvent B was 0.1% TFA in acetonitrile. Absorbance was measured at 230 nm.

residues in the proteins (Figure 1) (*23*). To determine whether all of these cysteine residues are involved in disulfide bridges, the purified native AFP was denatured in guanidine-HCl in the absence of reducing agent and exposed to iodoacetic acid at pH 8.8 to alkylate any free cysteine residues. The MALDI-TOF data showed that after this treatment there was no molecular weight change of this protein compared with that of the native AFP, indicating a lack of free cysteine residues in these proteins. Thus all the 16 cysteine residues are involved in disulfide bridges.

Figure 3 shows the RP-HPLC chromatography of the pepsin digestion mixture of AFP. Peptide 14.73 in Figure 3 was rechromatographed (Figure 4A). After reduction, only one peptide (retention time of 15.02 min) was obtained (Figure 4B). The first 7 cycles of Edman degradation of this peptide yielded KAKTCTG, while MALDI-TOF analysis indicated that this fragment has a molecular weight of

Table 1: Summary of Results of Peptide and Disulfide Mapping

peptide fragment from Figure 3	reduction state	peptide fragments after reduction	MS_{obs}[a]	MS_{cal}[a]	Edman degradation	identified peptides and disulfides
14.73	reduced	15.02	1477.11	1476.77	KAKTCTG	^{60}KAKTCTGSTNCYEA^{73}
13.12	unreduced		1046.19 1274.15			
	reduced	13.32 (dominant)	1047.61	1048.19	TCTRS	^{51}TCTRSTNCY^{59}
	reduced	14.20	1275.77	1276.88	KAKTC	^{60}KAKTCTGSTNCY^{71}
15.94	unreduced		1393.33 1568.93			
	reduced	15.90	1396.78	1396.62	RTACTR	^{25}RTACTRSSNCINA^{37}
	reduced	19.05 (dominant)	1571.68	1572.61	LTCTDS	^{38}LTCTDSYDCHNAET^{51}
5.96	reduced	5.96	1394.74	1394.42	RTACTR	^{25}RTACTRSSNCNNA^{37}
15.50	unreduced		1395.78 1471.76			
	reduced	15.49 (dominant)	1394.75	1396.62	RTACTR	^{25}RTACTRSSNCINA^{37}
	reduced	18.20	1471.63	1471.58	LTCTD	^{38}LTCTDSYDCHNAE^{50}
B	reduced	B	952.17	953.06	TACTD	^{74}TACTDSTGCP^{83}
4.15	reduced	4.15	780.85	779.62	CTDSTG	^{76}CTDSTGCP^{83}

[a] MS_{cal}= Calculated mass of the peptide. MS_{obs} = MALDI-TOF mass.

1477.11. By comparison with the known sequence of the AFP (Figure 1), it was found that this is the peptide fragment ^{60}KAKTCTGSTNCYEA^{73} with a calculated molecular weight of 1476.77.

This peptide fragment unambiguously identifies a disulfide between C65 and C71. (Table 1 presents a summary of these, and subsequent, data.)

Peptide 13.12 from the pepsin digestion in Figure 3 was rechromatographed. After reduction, two fragments were obtained (Figure 5A). For peptide 13.32, the first 5 cycles of Edman degradation yielded TCTRS, while MALDI-TOF analysis indicated a molecular weight of 1047.61 (Table 1). For peptide 14.20, the first 5 cycles of Edman degradation yielded KAKTC with a molecular weight of 1275.77 by MALDI-TOF. By comparison with the known sequence, it was found that these corresponded respectively to peptide 13.32, ^{51}TCTRSTNCY^{59}, with a calculated molecular weight of 1048.19, and peptide 14.20, ^{60}KAKTCTGSTNCY^{71} with a calculated molecular weight of 1276.88 (Table 1).

There are two possibilities for the disulfide linkage pattern involving these two peptides. One possibility is that each peptide has an intrachain disulfide. This is in agreement with the peptide 14.73 disulfide mapping described above. The other possibility is that each cysteine in one peptide forms an interchain disulfide with another cysteine in the other peptide. However, it was obvious from Figure 5A that the intensity of these two reduced peptides is not 1:1, but rather peptide 14.20 is dominant even though both peptides contain one Tyr. If these two peptides are from reduced interchain disulfides, they should have an intensity ratio of approximately 1:1 instead of 1:10. Further evidence that interchain disulfides are impossible comes from the MALDI-TOF analysis of the unreduced peptide 13.12 which clearly indicated that it contains two fragments with molecular weights of 1274.15 and 1046.19, but no fragment of 2323.75 was detected (Figure 5B). Therefore, these two peptides appear to co-elute before reduction, and it was concluded

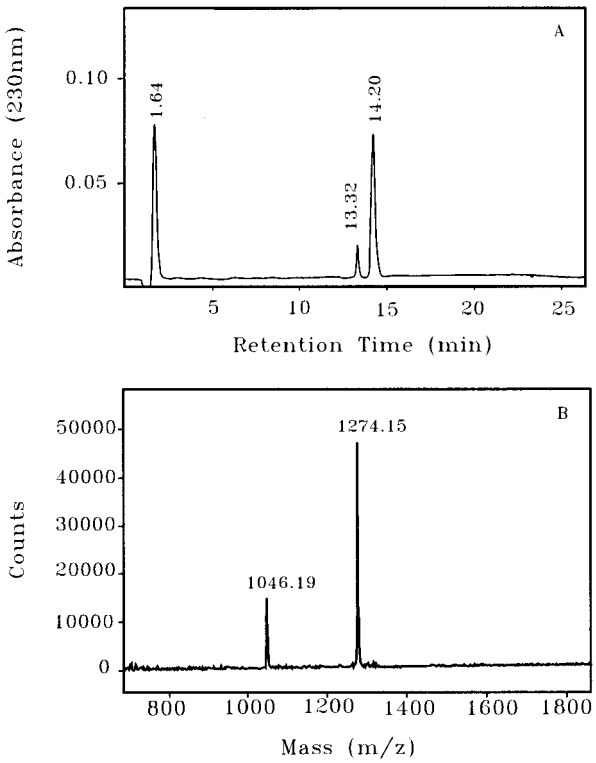

FIGURE 5: (A) Analysis of peptide 13.12 from Figure 3. Peptide 13.12 was purified to homogeneity by RP-HPLC rechromatography and speed-vacuum-dried. After reduction in 100 μL of 0.2 M sodium citrate, pH 3.0, by 15 mM TCEP at 60 °C for 20 min, it was chromatographed again by reverse-phase HPLC on a Rainin C18 column at a flow rate of 1.0 mL/min with a 5−30% linear gradient of solvent B in 40 min, where solvent A was 0.1% TFA in water and solvent B was 0.1% TFA in acetonitrile. Absorbance was measured at 230 nm. (B) MALDI-TOF analysis of peptide 13.12 from Figure 3 after repurification without reduction.

that peptides 13.32 and 14.20 respectively have the following linkage patterns (Table 1): ^{51}TCTRSTNCY^{59} and ^{60}KAKTCTGSTNCY^{71}.

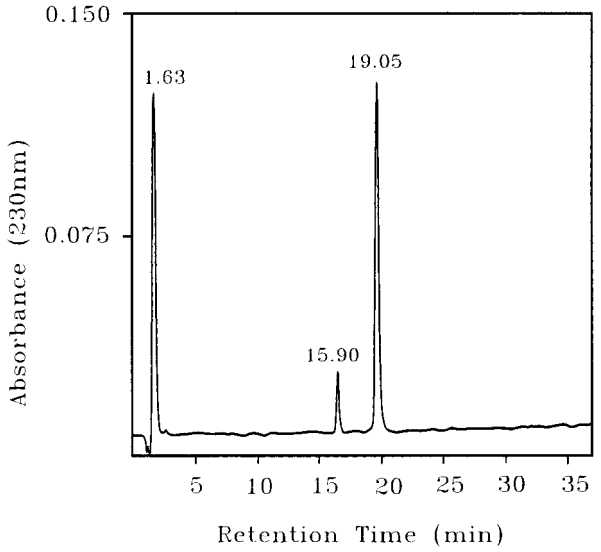

FIGURE 6: Analysis of peptide 15.94 from Figure 3. Peptide 15.94 was purified to homogeneity by HPLC rechromatography and speed-vacuum-dried. After reduction in 100 μL of 0.2 M sodium citrate, pH 3.0, by 15 mM TCEP at 60 °C for 20 min, it was rechromatographed again by reverse-phase HPLC on a Rainin C18 column at a flow rate of 1.0 mL/min with a 5−30% linear gradient of solvent B in 40 min, where solvent A was 0.1% TFA in water and solvent B was 0.1% TFA in acetonitrile. Absorbance was measured at 230 nm.

Peptide 15.94 from pepsin digestion in Figure 3 was rechromatographed. After reduction, two fragments, peptides 15.90 and 19.05, were obtained (Figure 6). For peptide 15.90, the first 6 cycles of Edman degradation yielded RTACTR, while the MALDI-TOF analysis indicated a molecular weight of 1396.78. For peptide 19.05, the first 6 cycles of Edman degradation yielded LTCTDS with a molecular weight of 1571.68. Again, by comparison with the known sequence, these peptides have the following sequences: peptide 15.90, ^{25}RTACTRSSNCINA^{37}, with a calculated molecular weight of 1396.62, and peptide 19.05, ^{38}LTCTDSYDCHNAET^{51}, with a calculated molecular weight of 1572.61.

MALDI-TOF analysis of the unreduced peptide 15.94 indicated that there were two species in the sample with molecular weights of 1393.33 and 1568.93, but no fragment with a molecular weight corresponding to the sum of the above two was detected. So each of these two peptides has an intrachain disulfide bridge as shown (Table 1): peptide 15.90, ^{25}RTACTRSSNCINA^{37}, and peptide 19.05, ^{38}LTCTDSYDCHNAET^{51}.

The intrachain disulfide of peptide 15.90 is supported by the mapping of peptide 5.96 in Figure 3. After reduction of peptide 5.96, only one fragment was obtained. Edman degradation (RTACTR) and MALDI-TOF analysis (1394.74) indicated that it is the fragment ^{25}RTA$\overline{\text{CTRSSNC}}$NNA^{37} with an interchain disulfide and a calculated molecular weight of 1394.42 (Table 1).

It is worthy to note here that the above peptide differs from peptide 15.90 only in that N_{35} replaced I so that the retention time of peptide 5.96 was substantially decreased. AFP-2 has this substitution (Figure 1). Therefore, peptide 15.90 is from AFP-1 and peptide 5.96 is from the same region of AFP-2.

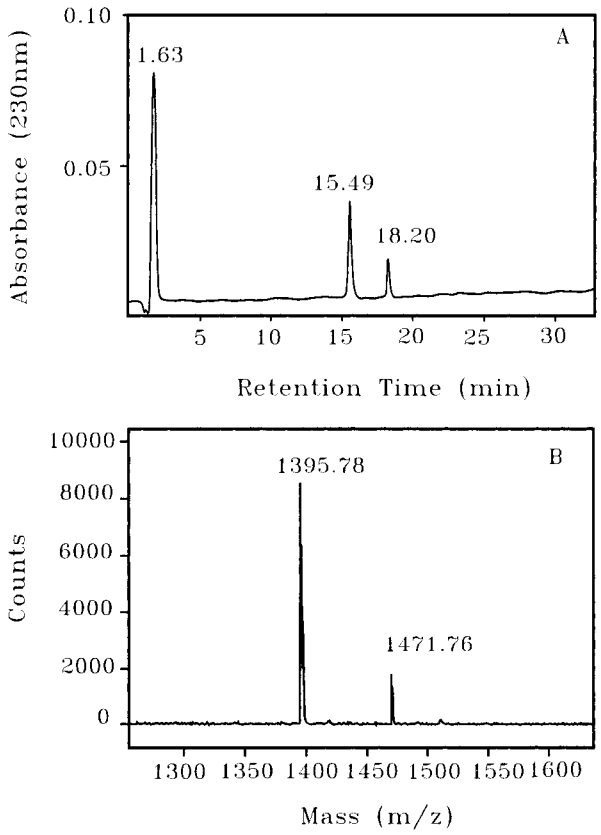

FIGURE 7: (A) Analysis of peptide 15.50 from Figure 3. Peptide 15.50 was purified to homogeneity by HPLC and speed-vacuum-dried. After reduction in 100 μL of 0.2 M sodium citrate, pH 3.0, by 15 mM TCEP at 60 °C for 20 min, it was chromatographed again by reverse-phase HPLC on a Rainin C18 column at a flow rate of 1.0 mL/min with a 5−30% linear gradient of solvent B in 40 min, where solvent A was 0.1% TFA in water and solvent B was 0.1% TFA in acetonitrile. Absorbance was measured at 230 nm. (B) MALDI-TOF analysis of peptide 15.50 from Figure 3 after repurification without reduction.

Peptide 15.50 from pepsin digestion in Figure 3 was rechromatographed, and after reduction, two peptides were obtained (Figure 7A). For peptide 15.49, the first 6 cycles of Edman degradation yielded RTACTR with a MALDI-TOF molecular weight of 1394.75. For peptide 18.20, the first 5 cycles of sequencing yielded LTCTD with a molecular weight of 1471.63. Comparison with the native sequence indicates that these peptides have the following sequences (Table 1): peptide 15.49, ^{25}RTACTRSSNCINA^{37}, with a calculated molecular weight of 1396.62, and peptide 18.20, ^{38}LTCTDSYDCHNAE^{50}, with a calculated molecular weight of 1471.58.

Again it was impossible for these two peptides to form interchain disulfides, for the following two reasons: (A) The molar ratio of these two peptides is far from 1:1 (Figure 7A). (Note that the intensity of peptide 18.20 has been greatly improved by the presence of one Tyr.) (B) On the mass spectrum of the unreduced peptide, only two species were identified (Figure 7B). Therefore, these two peptides each have an intrachain disulfide as follows (Table 1): peptide 15.49, ^{25}RTA$\overline{\text{CTRSSNC}}$INA^{37}, and peptide 18.20, ^{38}LTCTDSYDCHNAE^{50}.

Peptide B (retention time, ~7 min) from the pepsin digestion in Figure 3 gave a single peptide after reduction.

Peptide sequencing (TACTD) and mass data (952.17) (unreduced) showed that it was from the C-terminus with the sequence ^{74}TACTDSTGCP^{83} and a calculated molecular weight of 953.06. Thus, the C-terminus peptide has the intrachain disulfide ^{74}TACTDSTGCP^{83}.

This assignment was further supported by another peptide, 4.15, from the pepsin digestion in Figure 3 which gave only one peptide after reduction. Peptide sequencing (CTDST) and mass data (780.85) (unreduced) showed that it was also from the C-terminus with the sequence ^{76}CTDSTGCP^{83} and a calculated molecular weight of 779.62.

Peptide 17.46 from Figure 3 showed one peak after reduction, indicating that it was an intact peptide fragment without internal cleavage. Edman degradation failed to give any sequence information, which suggests that it was from the blocked N-terminus. Mass data revealed that this fragment has a molecular weight of 2429.03 (unreduced), consistent with the N-terminal peptide with a pyroglutamate at the N-terminus: p^{1}QCTGGSDCRSCTVSCTDCQNCP-NA^{24}, calculated molecular weight, 2429.79.

This peptide was further analyzed by partial reduction in which the peptide was transformed into a mixture of isoforms, each of which corresponds to reduction of only one of its disulfide bridges. After cyanylation of the free thiols of the cysteines by CDAP, each isoform was separated by RP-HPLC (Figure 8A). MS analysis indicates that peaks 19.70, 20.53, and A each had only one disulfide reduced. The pH of these samples was then adjusted to 12.0, causing cleavage at the N-terminal peptide bond of the cyanylated cysteinyl residue. Subsequently, the sample was fully reduced for MALDI-MS analysis (Figure 8B, C D). Results of these manipulations are summarized in Table 2.

The analysis of peak 19.70 by MALDI-TOF after base cleavage revealed two peptides with molecular weights of 910.577 and 1483.85, corresponding to reduction of the disulfide linkage between Cys 2 and Cys 11. The second fragment, the N-terminal pyroglutamate with a calculated molecular weight of 128, was too small to be detected by MALDI-TOF. MALDI-TOF analysis of peak 20.53 after base cleavage revealed two peptides with molecular weights of 774.64 and 1100.27, corresponding to reduction of the disulfide linkage of Cys 8 and Cys 18. The associated fragment (648.63) was not detected by MALDI-TOF due to the interference of matrix peaks. MALDI-TOF analysis of peak A found only one prominent peptide with a molecular weight of 1387.23, which forms upon reduction of the disulfide bridge between Cys 15 and Cys 21. The other two peptides were not seen due to matrix peak interference. These data are indicative of three disulfide bridges in the N-terminal fragment, between Cys 2 and Cys 11, between Cys 8 and Cys 18, and between Cys 15 and Cys 21, respectively.

Figure 9 summarizes the disulfide bridge mapping of AFP-1 from *Dendroides canadensis*. AFP-2 has the same pattern.

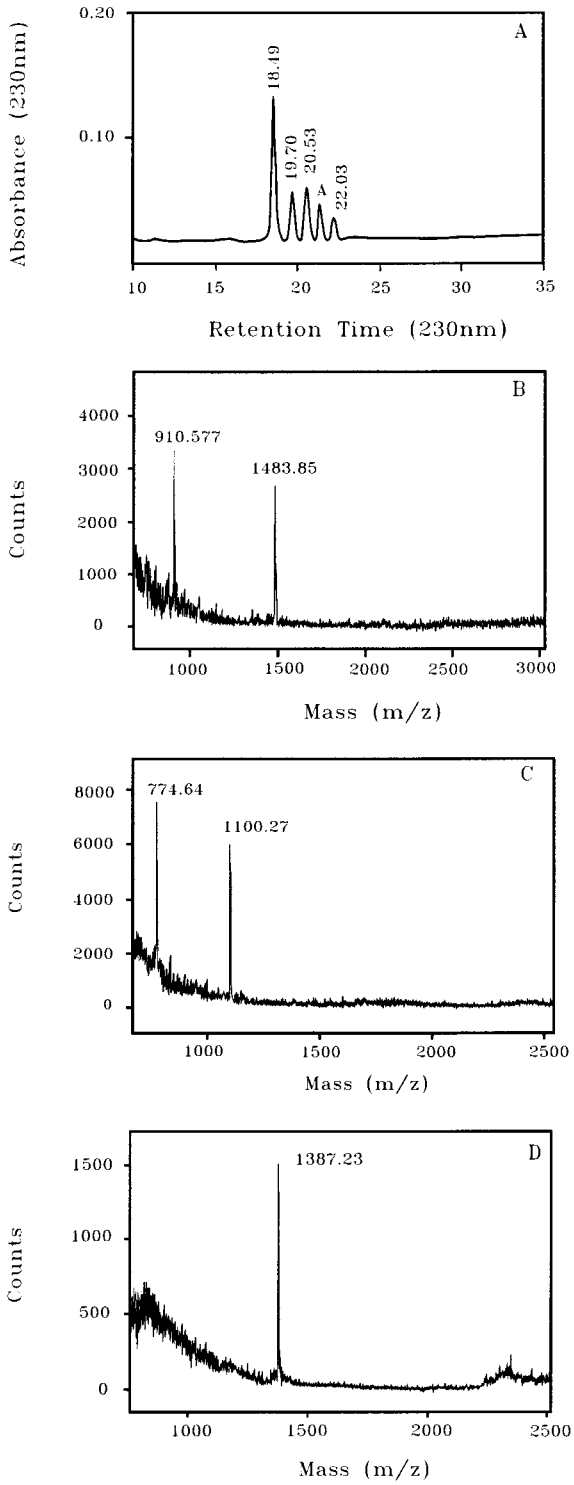

FIGURE 8: (A) RP-HPLC separation of peptide 17.46 from Figure 3 (N-terminal fragment) and its partially reduced/cyanylated isomers. Peptides were separated by reverse-phase HPLC on a Rainin C18 column at a flow rate of 1.0 mL/min with a 5−30% linear gradient of solvent B in 40 min, where solvent A was 0.1% TFA in water and solvent B was 0.1% TFA in acetonitrile. Absorbance was measured at 230 nm. The peak 18.49 is intact peptide. Peaks 19.70, 20.53, and A represent singly reduced/cyanylated isomers, as determined by MALDI-TOF analysis. (B, C, D) The MALDI mass spectra of peptide mixtures resulting from the cleavage of the singly reduced/cyanylated peptides. Panel B: Peptide 19.70 from Figure 8A. Panel C: Peptide 20.53 from Figure 8A. Panel D: Peptide A from Figure 8A.

DISCUSSION

The seven 12- or 13-mer repeating units present in the *Dendroides* AFPs (Figure 1), in combination with the seven disulfide bridges between the cysteines located every six residues throughout most of the length of the protein, is highly suggestive of the presence of seven functional domains in these AFPs (Figure 9). The additional disulfide

Table 2: Disulfide Bridge Mapping Based on the *m*/*z* of Fragments from the Base Cleavage of the N-terminal Peptide of the AFPs[a]

peptide	*m*/*z* from MALDI	fragments deduced	*m*/*z* calcd	disulfides opened
19.70	–	pQ[1]	128.14	Cys 2−Cys 11
	910.577	[2]CTGGSDCRS[10]	909.99	
	1483.85	[11]CTVSCTDCQNCPNA[24]	1483.53	
20.53	–	[1]QCTGGSD[7]	648.63	Cys 8−Cys 18
	1100.27	[8]CRSCTVSCTD[17]	1099.14	
	774.64	[18]CQNCPNA[24]	773.79	
A	1387.23	[1]QCTGGSDCRSCTVS[14]	1385.44	Cys15−Cys 21
	–	[15]CTDCQN[20]	707.69	
	–	[21]CPNA[24]	428.47	

[a] (−) indicates no *m*/*z* was obtained for that fragment due to matrix peak interference.

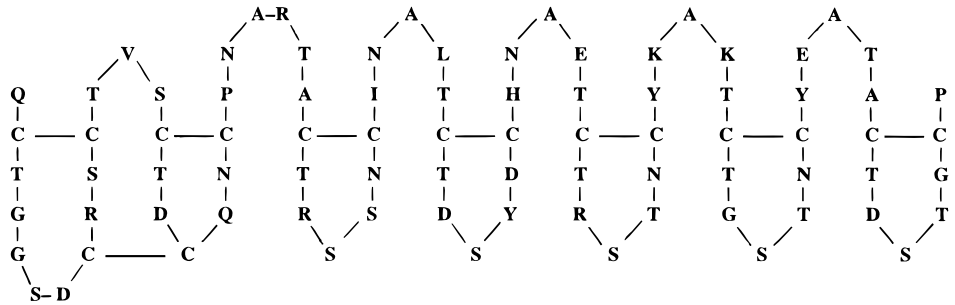

FIGURE 9: *Dendroides* AFP-1 sequence showing the location of the disulfide bridges.

linkage between Cys 8 and Cys 18 is the only "irregular" linkage, but note that these two cysteines located toward the N-terminus are the only cysteines whose spacing differs from the aforementioned normal six-residue spacing of the other cysteines. The function of this linkage between Cys 8 and Cys 18 is not obvious, but it may contribute to higher order structure near the N-terminus which is somewhat different from the rest of the protein.

Although the specific activities of the *Dendroides* AFPs are greater than those of the various fish AFPs (*5*), it is likely that the mechanism of action is similar to that suggested for fish AFPs (*19*−*22*, *26*). This involves a lattice match between certain residues of the AFP and water molecules of ice which then permits the adsorption of AFP, probably via hydrogen bonding, onto otherwise preferred growth sites of the ice crystal. The presence of the seven repeats with highly conserved positions within the 12−13-mers is consistent with this expected mechanism of action. It is likely that the regular disulfide bridges ensure the appropriate alignment of the hydroxyl side chains of the highly conserved threonine and serine residues, thereby providing the necessary lattice match and hydrogen bonding between the AFPs and ice.

As demonstrated previously (*24*), the *Dendroides* AFPs are unusually hydrophilic proteins. However, without knowing the higher order structure of these AFPs, inspection of Figure 9 suggests that it is likely that the *Dendroides* AFPs may present a somewhat hydrophobic region formed by the methyl groups of the alanines, along with the valine side chain, located on the upper edge of the AFP. In fact, essentially all of the hydrophobic residues are located in the half of the protein above the disulfide bridges as presented in Figure 9. In contrast, the other half of the protein is quite hydrophilic. This is somewhat reminiscent of the amphiphilic nature of the fish antifreeze glycoproteins and the type I fish antifreeze proteins, even though the sequences of the *Dendroides* AFPs and these fish AFPs are considerably different. The only fish AFPs with cysteines are the type II AFPs. The *Dendroides* AFPs are not similar to these type II fish AFPs since the fish and beetle AFPs lack sequence homology and the type II fish AFPs have fewer disulfide linkages (*5*) than do the beetle AFPs (*8*). Recently, the sequences of AFPs were determined from two other insects, the spruce budworm *Choristoneura fumiferana* (*27*) and the beetle *Tenebrio molitor* (*28*). While the spruce budworm AFP is not similar to that of *Dendroides canadensis*, the *Tenebrio molitor* AFPs have 48−67% identity with the *Dendroides* AFPs including exact matching of all the cysteine residues. Therefore, it is likely that the disulfide bridge locations presented here for the *Dendroides* AFPs also hold for the *Tenebrio molitor* AFPs.

Although the disulfide mapping presented in this study provides important information on the structure of the beetle AFPs, on the basis of existing information it is still not obvious why these beetle AFPs are so much more active than the known fish AFPs.

REFERENCES

1. DeVries, A. L. (1971) Glycoproteins as biological antifreeze agents in antarctic fishes. *Science 172*, 1152−1155.
2. DeVries, A. L., and Cheng, C.-H. C. (1992) The role of antifreeze glycopeptides and peptides in the survival of cold-water fishes. In *Water and Life* (Somero, G. N., Osmond, C. B., and Bolis, C. L., Eds.) pp 301−315, Springer-Verlad, Berlin.
3. Davies, P. L., and Hew, C. L. (1990) Biochemistry of fish antifreeze proteins. *FASEB J. 4*, 2460−2468.
4. Duman, J. G. (1977) The role of macromolecular antifreeze in the darkling beetle *Meracantha contract*. *J. Comp. Physiol. 115B*, 279−286.
5. Duman, J. G., Wu, D. W., and Olsen, T. M. (1993) Thermal-hysteresis proteins. *Adv. Low-Temp. Biol. 2*, 131−182.
6. Duman, J. G. (1979) Subzero temperature tolerance in spiders: The role of thermal hysteresis factors. *J. Comp. Physiol. 131*, 347−352.

7. Husby, J. A., and Zachariassen, Z. E. (1980) Antifreeze agents in the body fluid of winter active insects and spiders. *Experientia 36*, 963−964.
8. Block, W., and Duman, J. (1989) Presence of thermal hysteresis producing antifreeze proteins in the Antarctic mite, *Alaskozetes antarcticus. J. Exp. Zool. 250*, 229−231.
9. Tursman, D., Duman, J. G., and, C. A. (1994) Freeze tolerance adaptations in the centipede *Lithobius forficatus*. *J. Exp. Zool. 268*, 347−353.
10. Tursman, D., and Duman, J. G. (1995) Cryoprotective effects of thermal hysteresis protein on survivorship of frozen gut cells from the freeze tolerant centipede *Lithobius forficatus*. *J. Exp. Zool. 272*, 249−257.
11. Urrutia, M. E., Duman, J. G., and Knight, C. A. (1992) Plant thermal hysteresis proteins. *Biochim. Biophys. Acta 1121*, 199−206.
12. Griffith, M., Marentes, E., Ala, P., and Yang, D. S. C. (1992) The role of ice binding proteins in frost tolerance of winter rye. In *Advances in Plant Cold Hardiness* (Li, P. H., and Christersson, L., Eds.) pp 174−184, CRC Press, Boca Raton.
13. Griffith, M., Ala, P., Yang, D. S. C., Hon, W.-C., and Moffatt, B. A. (1992) Antifreeze protein produced endogenously in winter rye leaves. *Plant Physiol. 10*, 593−596.
14. Duman, J. G., and Olsen, T. M. (1993) Thermal hysteresis activity in bacteria, fungi and primitive plants. *Cryobiology 30*, 322−328.
15. Duman, J. G. (1994) Purification and characterization of thermal hysteresis proteins from a plant, the bittersweet nightshade, *Solanum dulcamara*. *Biochim. Biophys. Acta 1206*, 129−135.
16. Olsen, T. M., and Duman, J. G. (1997) Maintenance of the supercooled state in overwintering Pyrochroid beetle larvae *Dendroides canadensis*: role of hemolymph ice nucleators and antifreeze proteins. *J. Comp. Physiol. B 167*, 105−113.
17. Olsen, T. M., and Duman, J. G. (1997) Maintenance of the supercooled state in the gut of overwintering Pyrochroid beetle larvae, *Dendroides canadensis*: role of gut ice nucleators and antifreeze proteins. *J. Comp. Physiol. B 167*, 114−122.
18. DeVries, A. L. (1986) Antifreeze glycopeptides and peptides: Interactions with ice and water. *Methods Enzymol. 127*, 293−303.
19. Raymond, J. A., Radding, W., and DeVries, A. L. (1977) Circular dichroism of protein and glycoprotein fish antifreeze. *Biopolymers 16*, 2575−2578.
20. Raymond, J. A., Wilson, P. W., and DeVries, A. L. (1989) Inhibition of growth on nonbasal planes in ice by fish antifreeze. *Proc. Natl. Acad. Sci. U.S.A. 86*, 881−885.
21. Knight, C. A., Cheng, C. C., and DeVries, A. L. (1991) Adsorption of -helical antifreeze peptides on specific ice crystal surface planes. *Biophys. J. 59*, 409−418.
22. Sicheri, F., and Yang, D. S. C. (1995) Ice-binding structure and mechanism of an antifreeze protein from winter flounder. *Nature 375*, 427−431.
23. Duman, J. G., Li, N., Verleye, D., Goetz, F. W., Wu, D. W., Andorfer, C. A., Benjamin, T., and Parmalee, D. C. (1998) Molecular characterization and sequencing of antifreeze proteins from larvae of the beetle *Dendroides canadensis*. *J. Comp. Physiol. B* (in press).
24. Wu, D. W., Duman, J. G., Cheng, C.-H. C., and Castellino, F. J. (1991) Purification and characterization of antifreeze proteins from larvae of the beetle *Dendroides canadensis*. *J. Comp. Physiol. 161*, 271−278.
25. Wu, J., Gage, D. A., and Watson, J. T. (1996) A strategy to locate cysteine residues in proteins by specific chemical cleavage followed by matrix-assisted laser desorption/ionization time-of-flight mass spectrometry. *Anal. Biochem. 235*, 161−174.
26. Wilson, P. W. (1993) Explaining thermal hysteresis by the Kelvin effect. *Cryo. Lett. 14*, 31−36.
27. Tyshenko, M. G., Doucet, D., Davies, P. L., and Walker, V. K. (1997) The antifreeze potential of the spruce budworm thermal hysteresis protein. *Nature Biotechnol. 15*, 887−890.
28. Graham, L. A., Liou, Y.-C, Walker, V. K., and Davies P. L. (1997) Hyperactive antifreeze protein from beetles. *Nature 388*, 727−728.

BI972853I